

# Exploring Hyperchargeless Higgs Triplet Model up to the Planck Scale

Najimuddin Khan<sup>1,\*</sup>

<sup>1</sup>*Discipline of Physics, Indian Institute of Technology Indore,  
Khandwa Road, Simrol, Indore - 453 552, India*

## Abstract

We examine extended Higgs triplet of Standard Model taking into consideration the Higgs-like particle discovery at the LHC with mass around 125 GeV. We evaluate the bounds on the scalar potential through the unitarity of the scattering-matrix. Considering with and without  $Z_2$ -symmetry on the extra triplet, we derive constraints on the parameter space. We identify the region of the parameter space that corresponds to the stability and metastability of the electroweak vacuum.

---

\* phd11125102@iiti.ac.in

## I. INTRODUCTION

The revelation of the Higgs boson [1–3] on 2012 at the Large Hadron Collider (LHC), confirmed the existence of all Standard Model (SM) particles and the Higgs mechanism to be responsible for electroweak symmetry breaking (EWSB). The values of all the SM parameters in the Lagrangian are known at the electroweak (EW) scale. So far, the LHC, operated with pp collision energy at  $\sqrt{s} \sim 8$  and 13 TeV or other experiments have not found any signature of new physics beyond the standard model (BSM). However, various theoretical issues, like the hierarchy problem related to the mass of the Higgs, mass hierarchy and mixing patterns in leptonic and quark sectors and the experimental observations, such as non-zero neutrino mass, baryon-antibaryon asymmetry in the Universe, mysterious nature of dark matter (DM) and dark energy have indicated the new physics beyond the SM. Also, the measured properties of the Higgs boson with mass  $\sim 125$  GeV are consistent with the minimal choice of the scalar doublet as predicted by the SM. But the experimental data [4] obtained by the LHC, still comfortably allow extra scalar particles as a singlet, doublet or triplet, etc. under  $SU(2)_L$ , which may also be responsible for the EWSB.

The experimental values of the SM parameter of the Lagrangian indicate that if the validity of the SM is extended to Planck scale ( $M_{\text{Pl}} = 1.2 \times 10^{19}$  GeV), a second, deeper minimum is located near the Planck scale such that, the EW vacuum is metastable, i.e., the transition lifetime of the EW vacuum to the deeper minimum is finite  $\tau_{EW} \sim 10^{300}$  years [5–10]. The EW vacuum remains metastable state even after adding extra scalar particles in the SM, which has been discussed in Refs. [5, 6].

In this work, we add a real hypercharge  $Y = 0$  scalar triplet with the SM. In the literature, this model is termed as the hyperchargeless Higgs triplet model, HTM ( $Y = 0$ ) [11]. We consider both the neutral  $CP$ -even component of the SM doublet and the extra scalar triplet take part in the EWSB [12]. We study for the first time of the parameter space of HTM ( $Y = 0$ ) by including radiative corrections, which valid up to the Planck scale ( $M_{\text{Pl}}$ ). The structure of the scalar potential in this new model and, how the new scalar fields interact with the SM particles and between one another is discussed. Various theoretical and experimental bounds on this model are reviewed. We especially discuss the unitary bounds. To the best of our knowledge, the unitary bounds in this model were not discussed in the literature. Next, we impose a  $Z_2$ -symmetry on the extra scalar particle such that an *odd* number of scalar fields of the triplet do not couple with the SM particles. The lightest neutral scalar particle does not decay and becomes stable. This scalar field can be taken as a viable DM candidate which may fulfill the relic abundance of the Universe. In this context, it is instructive to explore whether these extra scalars can also extend the lifetime of the Universe. We found the new parameter spaces in this model for which the EW vacuum still remain metastable. We have identified the region of parameter spaces for which the EW vacuum

becomes stable and metastable.

A detailed study of the HTM ( $Y = 0$ ) parameter space, valid up to 1 TeV, has been done in Refs.[13]. Renormalization scheme, electroweak precision, and decoupling of Higgs triplet scenario has been discussed in Ref.[14]. In Refs.[15–18], using EWPT data, including one-loop correction to the  $\rho$  parameter, had predicted the range of the Higgs mass. Authors of Ref.[19] have studied the detailed vacuum structure of the scalar potential at tree-level. Constraints on the parameter spaces from recent  $\mu_{\gamma\gamma}$  and  $\mu_{Z\gamma}$  data from LHC has been discussed in Ref. [20]. The detailed DM constraints on this model recently have been studied in Refs. [21–24].

The paper is organized as follows. Section II starts with an detailed descriptions of HTM ( $Y = 0$ ) model. We discuss detailed constraints in Sec. III. Considering the lightest neutral  $Z_2$ -odd particle of HTM as a DM candidate, we analyzed the scalar potential up to the Planck scale and study the parameter space identifying regions of EW vacuum stability and metastability in Sec. IV. Finally we conclude in Sec. V.

## II. MODEL

We consider a model with a real Higgs doublet,  $\Phi$ , and a real, isospin  $I = 1$ , hypercharge  $Y = 0$  triplet  $T$ . The extra scalar triplet consists of a pair of singly-charged fields and a  $CP$ -even neutral scalar field. The doublet and triplet scalar are conventionally written as [14],

$$\Phi = \begin{pmatrix} G_1^+ \\ \frac{1}{\sqrt{2}}(v_1 + h^0 + iG^0) \end{pmatrix}, \quad T = \begin{pmatrix} \eta^+ \\ v_2 + \eta^0 \\ -\eta^- \end{pmatrix}. \quad (2.1)$$

The kinetic part of the Lagrangian is given by,

$$\mathcal{L}_k = |D_\mu \Phi|^2 + \frac{1}{2} |D_\mu T|^2, \quad (2.2)$$

where the covariant derivatives are defined as,

$$D_\mu \Phi = \left( \partial_\mu + i\frac{g_2}{2}\sigma^a W^a + i\frac{g_1}{2}Y B_\mu \right) \Phi \quad \text{and} \quad D_\mu T = \left( \partial_\mu + ig_2 t_a W^a \right) T, \quad (2.3)$$

where,  $W_\mu^a$  ( $a=1,2,3$ ) are the  $SU(2)_L$  gauge bosons, corresponding to three generators of  $SU(2)_L$  group and  $B_\mu$  is the  $U(1)_Y$  gauge boson.  $\sigma^a$  ( $a = 1, 2, 3$ ) are the Pauli matrices, and  $t_a$  can be written as follows,

$$t_1 = \frac{1}{\sqrt{2}} \begin{pmatrix} 0 & 1 & 0 \\ 1 & 0 & 1 \\ 0 & 1 & 0 \end{pmatrix}, \quad t_2 = \frac{1}{\sqrt{2}} \begin{pmatrix} 0 & -i & 0 \\ i & 0 & -i \\ 0 & i & 0 \end{pmatrix}, \quad t_3 = \begin{pmatrix} 1 & 0 & 0 \\ 0 & 0 & 0 \\ 0 & 0 & -1 \end{pmatrix}. \quad (2.4)$$

The scalar potential is such that both the neutral  $CP$ -even component of the SM doublet and the extra scalar triplet receive vacuum expectation value (VEV), take part in the EWSB. After EWSB, one of the linear combination of charged scalar fields of scalar doublet and the triplet is eaten by the  $W$  boson which becomes massive, other orthogonal combinations of these fields become massive charged scalar fields. Similarly, a pseudoscalar of scalar doublet become the longitudinal part of massive  $Z$  gauge boson. This scalar may give rise a signature through vector bosons scatterings [12] in the collider experiments. The spontaneous EWSB generates masses for the  $W$  and  $Z$  bosons as,

$$M_W^2 = \frac{g_2^2}{4} (v_1^2 + 4v_2^2), \quad \text{and} \quad M_Z^2 = \frac{g_2^2}{4c_\theta^2} v_1^2,$$

where,  $c_W \equiv \cos \theta_W = g_2 / \sqrt{(g_1)^2 + (g_2)^2}$  and  $s_W \equiv \sin \theta_W$ . The VEVs  $v_1$  of the scalar doublet and  $v_2$  of the triplet are related to the SM VEV by  $v_{SM} (\equiv 246.221 \text{ GeV}) = \sqrt{v_1^2 + 4v_2^2}$ .

One can see that this model violates custodial symmetry at tree level,

$$\rho = \frac{M_W^2}{M_Z^2 c_W^2} = 1 + 4 \frac{v_2^2}{v_1^2}. \quad (2.5)$$

The experimental value of  $\rho$  is  $1.0004 \pm 0.00024$  [25] at  $1\sigma$ . Hence,  $\delta\rho \approx 0.0004 \pm 0.00024$  and we will adopt the bound  $\delta\rho \leq 0.001$ . This puts a stringent constraints on  $v_2$  and we get  $v_2$  should be less than 4 GeV.

The tree-level scalar potential with a Higgs doublet and a real scalar triplet invariant under  $SU(2)_L \times U(1)_Y$  transformation and is given by,

$$\begin{aligned} V(\Phi, T) = & \mu_1^2 |\Phi|^2 + \frac{\mu_2^2}{2} |T|^2 + \lambda_1 |\Phi|^4 + \frac{\lambda_2}{4} |T|^4 \\ & + \frac{\lambda_3}{2} |\Phi|^2 |T|^2 + \lambda_4 \Phi^\dagger \sigma^a \Phi T_a. \end{aligned} \quad (2.6)$$

We have the following minimization conditions of the tree-level scalar potential,

$$\begin{aligned} \mu_1^2 &= \frac{1}{2} \{2\lambda_4 v_2 - (2\lambda_1 v_1^2 + \lambda_3 v_2^2)\}, \\ \mu_2^2 &= \frac{1}{2v_2} \{\lambda_4 v_1^2 - \lambda_3 v_1^2 v_2 - 2\lambda_2 v_2^3\}. \end{aligned}$$

After electroweak symmetry breaking, the squared mass matrix can be expressed as  $6 \times 6$  for the scalar fields ( $G_1^\pm, \eta^\pm, \eta^0$  and  $h^0$ ). This matrix composed of three  $2 \times 2$  submatrices with bases, ( $G_1^+, \eta^+$ ), ( $G_1^-, \eta^-$ ) and ( $h^0, \eta^0$ ). After rotating these fields into the mass basis, we get four physical mass eigenstates ( $H^\pm, h, H$ ). The remaining two states ( $G^\pm$ ) and  $G^0$  become the massless Goldstone bosons.

The physical mass of the particles are given by,

$$\begin{aligned} M_h^2 &= \frac{1}{2} \left[ (B + A) - \sqrt{(B - A)^2 + 4C^2} \right], \\ M_H^2 &= \frac{1}{2} \left[ (B + A) + \sqrt{(B - A)^2 + 4C^2} \right], \\ M_{H^\pm}^2 &= \lambda_4 \frac{(v_1^2 + 4v_2^2)}{2v_2}, \end{aligned} \quad (2.7)$$

where,

$$A = 2\lambda_1 v_1^2, \quad B = \frac{\lambda_4 v_1^2 + 4\lambda_2 v_2^3}{2v_2}, \quad \text{and} \quad C = -\lambda_4 v_1 + \lambda_3 v_1 v_2. \quad (2.8)$$

The mixing between the doublet and triplet in the charged and  $CP$ -even scalar sectors are respectively given by,

$$\begin{pmatrix} h \\ H \end{pmatrix} = \begin{pmatrix} c_\gamma & s_\gamma \\ -s_\gamma & c_\gamma \end{pmatrix} \begin{pmatrix} h^0 \\ \eta^0 \end{pmatrix}, \quad (2.9)$$

$$\begin{pmatrix} G^\pm \\ H^\pm \end{pmatrix} = \begin{pmatrix} c_\beta & s_\beta \\ -s_\beta & c_\beta \end{pmatrix} \begin{pmatrix} G_1^\pm \\ \eta^\pm \end{pmatrix}, \quad (2.10)$$

where,

$$s_\gamma (\equiv \sin \gamma) = \sqrt{\frac{\sqrt{(B - A)^2 + 4C^2} - (B - A)}{2\sqrt{(B - A)^2 + 4C^2}}} \quad \text{and} \quad \tan \beta = \frac{2v_2}{v_1}.$$

In large  $\mu_2^2$  and small  $v_2$  limit one can express  $\sin \gamma$  and  $\sin \beta$  as,

$$s_\gamma = \sqrt{\frac{1}{2} - \frac{1}{2\sqrt{1 + 16\frac{v_2^2}{v_1^2}}}} \approx 0 \quad \text{and} \quad s_\beta = \frac{2v_2}{\sqrt{v_1^2 + 4v_2^2}} \approx 0.$$

In these limit the  $\lambda$ 's look like,

$$\lambda_1 = \frac{M_h^2}{2v_1^2}, \quad \lambda_2 = \frac{2(M_H^2 - M_{H^\pm}^2)}{v_1^2 s_\beta^2}, \quad \lambda_3 = \frac{2(M_{H^\pm}^2 - (s_\gamma/s_\beta)M_H^2)}{v_1^2}, \quad \lambda_4 = \frac{s_\beta M_{H^\pm}^2}{v_1^2}.$$

Also, in the same limit, if  $M_{H^\pm}$  and  $M_H$  are very heavy compared to  $M_h$ , then both the charged and heavy neutral particle masses should be degenerate (see eqns. 2.7 and 2.8). For large differences in  $M_{H^\pm}$  and  $M_H$ , the  $\lambda_{2,3}$  become non-perturbative (see subsection III B), or it may violate the unitarity (see subsection III C) conditions.

The SM gauge symmetry  $SU(2)_L$  prohibits direct coupling of SM fermions with the scalar fields of the triplet. The couplings of the new scalar fields ( $H, H^\pm$ ) with SM fermions is generated after the EWSB. The strength of  $H\bar{f}f$  ( $f$  are the  $up$ -,  $down$ -quarks and charged leptons) are proportional to  $\sin \gamma$ . Whereas  $H^+\bar{\nu}_l l^-$  and  $H^+\bar{u}d$  are proportional to  $\sin \beta$ .

### III. CONSTRAINTS ON HTM MODEL

The parameter space of this model is constrained by theoretical considerations like absolute vacuum stability, perturbativity, and unitarity of the scattering matrix. In the following, we will discuss these theoretical bounds and the bounds from the Higgs to diphoton signal strength at LHC and the electroweak precision measurements on the HTM ( $Y = 0$ ).

#### A. Vacuum stability bounds

A necessary condition for the stability of the vacuum comes from requiring that the scalar potential is bounded from below, i.e, it should not approach negative infinity along any direction of the field space at large field values. At the tree-level scalar potential  $V(\Phi, T)$  is bounded from below if

$$\lambda_1(\Lambda) \geq 0, \quad \lambda_2(\Lambda) \geq 0, \quad \lambda_3(\Lambda) \geq -2 \sqrt{\lambda_1(\Lambda)\lambda_2(\Lambda)}, \quad (3.1)$$

where,  $\Lambda$  is an arbitrary energy scale. If the quantum corrections are included to the scalar potential, then the above conditions will be more complicated. The modification of the stability conditions of the scalar potential will be shown in Subsection IV B.

#### B. Perturbativity bounds

To ensure that the radiatively improved scalar potential  $V(\Phi, T)$  of the HTM ( $Y = 0$ ) remains perturbative at any given energy scale, one must impose the following upper bounds on the couplings  $\lambda$ 's of scalar potential  $V(\Phi, T)$  as,

$$|\lambda_{1,2,3}| \leq 4\pi \quad \text{and} \quad \left| \frac{\lambda_4}{\Lambda} \right| \leq 4\pi. \quad (3.2)$$

This translates into upper bounds on the running couplings at the energy scale  $\Lambda$ .

#### C. Unitarity bounds

Unitarity bound on the extended scalar sectors can be calculated from the scattering-matrix (S-matrix) of different processes. The technique was developed by Benjamin W. Lee, C. Quigg, and H. B. Thacker for the SM and it can also be applied to the HTM ( $Y = 0$ ). The S-matrix for the HTM ( $Y = 0$ ) consists of different scalar-scalar, gauge boson-gauge boson, gauge boson-scalar scattering

amplitudes. Using the Born approximation for partial waves, the scattering cross-section for any process can be written as,

$$\sigma = \frac{16\pi}{s} \sum_l^{\infty} (2l+1) |a_l(s)|^2,$$

where,  $s = 4E_{CM}^2$  is the Mandelstam variable,  $E_{CM}$  is the center of mass energy of the incoming particles.  $a_l$  is the partial wave coefficients corresponding to specific angular momentum values  $l$ . This leads to the following unitarity constraint,  $Re(a_l) < \frac{1}{2}$ . At high energy the dominant contribution to the  $a_l$ , i.e., to the amplitude of the two-body scattering processes  $a, b \rightarrow c, d$  comes from the diagram involving the quartic couplings. Far away from the resonance, the other contributions to the amplitude from the scalar mediated  $s$ -,  $t$ -, and  $u$ -channel processes are negligibly small. Also in the high energy limit, the amplitude of scattering process involving longitudinal gauge bosons can be approximated by the scalar amplitude in which gauge bosons are replaced by their corresponding Goldstone bosons, e.g., the amplitude of  $W_L^+ W_L^- \rightarrow W_L^+ W_L^-$  scattering is approximated by  $G^+ G^- \rightarrow G^+ G^-$ . This is known as equivalence theorem [26, 27]. So to test unitarity of HTM ( $Y = 0$ ), we construct the S-matrix which consists of only the quartic couplings.

The scalar quartic couplings in the physical bases,  $G^\pm$ ,  $G^0$ ,  $H^\pm$ ,  $h$ ,  $H$ , are complicated functions of  $\lambda$ 's,  $\gamma$ ,  $\beta$ . For example, the  $hhhh$  vertex is  $6(\lambda_1 \cos^4 \gamma + \lambda_3 \cos^2 \gamma \sin^2 \gamma + \lambda_2 \sin^4 \gamma)$ . It is difficult to calculate the unitary bounds in the physical bases. So to simplify the quartic coupling, one can consider the non-physical scalar fields before the EWSB,  $G_1^\pm$ ,  $\eta^\pm$ ,  $G^0$ ,  $h^0$ ,  $\eta^0$ . Here the crucial point is that the S-matrix expressed in terms of the physical fields can be transformed into an S-matrix for the non-physical fields by making a unitary transformation [28, 29].

Different quartic couplings in non-physical bases obtained by expanding the scalar potential of eqn. 2.6, are given by,

$$\begin{aligned} \{G^0 G^0 G^0 G^0\} &= 6\lambda_1, & \{G^0 G^0 G_1^+ G_1^-\} &= 2\lambda_1, \\ \{G_1^+ G_1^+ G_1^- G_1^-\} &= 4\lambda_1, & \{G^0 G^0 h^0 h^0\} &= 2\lambda_1, \\ \{G_1^+ G_1^- h^0 h^0\} &= 2\lambda_1, & \{h^0 h^0 h^0 h^0\} &= 6\lambda_1, \\ \{G^0 G^0 \eta^0 \eta^0\} &= \lambda_3, & \{G_1^+ G_1^- \eta^0 \eta^0\} &= \lambda_3, \\ \{h^0 h^0 \eta^0 \eta^0\} &= \lambda_3, & \{\eta^0 \eta^0 \eta^0 \eta^0\} &= 6\lambda_2, \\ \{G^0 G^0 \eta^+ \eta^-\} &= \lambda_3, & \{G_1^+ G_1^- \eta^+ \eta^-\} &= \lambda_3, \\ \{h^0 h^0 \eta^+ \eta^-\} &= \lambda_3, & \{\eta^0 \eta^0 \eta^+ \eta^-\} &= 2\lambda_2, \\ & & \{\eta^+ \eta^+ \eta^- \eta^-\} &= 4\lambda_2. \end{aligned} \tag{3.3}$$

The full set of these non-physical scalar scattering processes can be expressed as a  $16 \times 16$  S-matrix.

This matrix is composed of three submatrices of dimensions  $6 \times 6$ ,  $5 \times 5$ , and  $5 \times 5$  which have different initial and final states.

The first  $6 \times 6$  sub-matrix  $\mathcal{M}_1$  corresponds to scattering processes whose initial and final states are one of these:  $(h^0 G_1^+, G^0 G_1^+, \eta^0 G_1^+, h^0 G_1^+, G^0 \eta^+, \eta^0 \eta^+)$ . Using the Feynman rules in eqn. 3.3, one can obtain  $\mathcal{M}_1$  as,  $\mathcal{M}_1 = \text{diag}(2\lambda_1, 2\lambda_1, 2\lambda_1, \lambda_3, \lambda_3, \lambda_3)$ .

The sub-matrix  $\mathcal{M}_2$  corresponds to scattering process with one of the following initial and final states:  $(h^0 G^0, G_1^+ \eta^-, \eta^+ G_1^-, \eta^0 G^0, h^0 \eta^0)$ . Similarly, one can calculate  $\mathcal{M}_2$ , it take the following form:  $\mathcal{M}_2 = \text{diag}(2\lambda_1, \lambda_3, \lambda_3, \lambda_3, \lambda_3)$ .

The third sub-matrix corresponds to scattering with one of the following initial and final states  $(G_1^+ G_1^-, \eta^+ \eta^-, \frac{G^0 G^0}{\sqrt{2}}, \frac{h^0 h^0}{\sqrt{2}}, \frac{\eta^0 \eta^0}{\sqrt{2}})$ . The factor  $\frac{1}{\sqrt{2}}$  appeared due to statistics of identical particles. So one can find  $\mathcal{M}_3$  with the help of the Feynman rules in eqn. 3.3 and is given by,

$$\mathcal{M}_3 = \begin{pmatrix} 4\lambda_1 & \lambda_3 & \sqrt{2}\lambda_1 & \sqrt{2}\lambda_1 & \frac{\lambda_3}{\sqrt{2}} \\ \lambda_3 & 4\lambda_2 & \frac{\lambda_3}{\sqrt{2}} & \frac{\lambda_3}{\sqrt{2}} & \sqrt{2}\lambda_2 \\ \sqrt{2}\lambda_1 & \frac{\lambda_3}{\sqrt{2}} & 3\lambda_1 & \lambda_1 & \frac{\lambda_3}{2} \\ \sqrt{2}\lambda_1 & \frac{\lambda_3}{\sqrt{2}} & \lambda_1 & 3\lambda_1 & \frac{\lambda_3}{2} \\ \frac{\lambda_3}{\sqrt{2}} & \sqrt{2}\lambda_2 & \frac{\lambda_3}{2} & \frac{\lambda_3}{2} & 3\lambda_2 \end{pmatrix}.$$

Eigenvalues of  $\mathcal{M}_3$  are:  $\left\{ 2\lambda_1, 2\lambda_1, 2\lambda_2, \frac{1}{2} \left( 6\lambda_1 + 5\lambda_2 \pm \sqrt{(6\lambda_1 - 5\lambda_2)^2 + 12\lambda_3^2} \right) \right\}$ .

Unitary constraints of the scattering processes demand that the eigenvalues  $e_i$ 's ( $i=1,..16$ ) of the S-matrix should be less than  $8\pi$ .

#### D. Bounds from electroweak precision experiments

Electroweak precision data has imposed severe bounds on new physics models via Peskin-Takeuchi [30]  $S$ ,  $T$ ,  $U$  parameters. The additional contributions from this model are given by [13, 18],

$$\begin{aligned} S &\simeq 0, \\ T &= \frac{1}{8\pi} \frac{1}{\sin^2 \theta_W \cos^2 \theta_W} \left[ \frac{M_H^2 + M_{H^\pm}^2}{M_Z^2} - \frac{2M_{H^\pm}^2 M_H^2}{M_Z^2 (M_H^2 - M_{H^\pm}^2)} \log \left( \frac{M_H^2}{M_{H^\pm}^2} \right) \right] \\ &\simeq \frac{1}{6\pi} \frac{1}{\sin^2 \theta_W \cos^2 \theta_W} \frac{(\Delta M)^2}{M_Z^2}, \\ U &= -\frac{1}{3\pi} \left( M_H^4 \log \left( \frac{M_H^2}{M_{H^\pm}^2} \right) \frac{(3M_{H^\pm}^2 - M_H^2)}{(M_H^2 - M_{H^\pm}^2)^3} + \frac{5(M_H^4 + M_{H^\pm}^4) - 22M_{H^\pm}^2 M_H^2}{6(M_H^2 - M_{H^\pm}^2)^2} \right) \end{aligned}$$



$$\simeq \frac{\Delta M}{3\pi M_{H^\pm}},$$

where  $\Delta M = M_{H^\pm} - M_H$ .  $S$  is proportional to  $\sin \beta$ . In the limit  $\beta \rightarrow 0$ , the contribution to the  $S$  parameter from the triplet scalar fields is negligible. For  $\beta \rightarrow 0$  and  $M_{H^\pm, H} \gg M_h$  the charged particle  $H^\pm$  and heavier  $CP$ -even Higgs  $H$  are almost degenerate in mass, i.e.,  $\Delta M$  is very small. Also the contributions to the  $T$  and  $U$  parameters [31] from this model are negligible.

### E. Bounds from LHC diphoton signal strength

Higgs to diphoton signal strength  $\mu_{\gamma\gamma}$  in the HTM ( $Y = 0$ ) is defined as,

$$\mu_{\gamma\gamma} = \frac{\sigma(gg \rightarrow h \rightarrow \gamma\gamma)_{\text{HTM}}}{\sigma(gg \rightarrow h \rightarrow \gamma\gamma)_{\text{SM}}} \approx \frac{\text{Br}(h \rightarrow \gamma\gamma)_{\text{HTM}}}{\text{Br}(h \rightarrow \gamma\gamma)_{\text{SM}}}. \quad (3.4)$$

As  $\frac{\Gamma_h^{\text{total}}}{M_h} \rightarrow 0$ , we can use the narrow width approximation for production cross-section of  $\sigma(gg \rightarrow h \rightarrow \gamma\gamma)$ . The production cross-section of  $h$ ,  $\sigma(gg \rightarrow h)$  in both the SM and HTM are the same. If the extra scalar particles ( $HT = H, H^\pm$ ) have masses greater than  $M_h/2$ , i.e.,  $\Gamma(h \rightarrow \text{HT}, \text{HT}) = 0$  then,

$$\mu_{\gamma\gamma} = \frac{\Gamma(h \rightarrow \gamma\gamma)_{\text{HTM}}}{\Gamma(h \rightarrow \gamma\gamma)_{\text{SM}}}. \quad (3.5)$$

In HTM, the additional contributions to  $\Gamma(h \rightarrow \gamma\gamma)$  at one-loop due to the  $H^\pm$  is given by [32],

$$\Gamma(h \rightarrow \gamma\gamma)_{\text{HTM}} = \frac{\alpha^2 M_h^3}{256\pi^3 v^2} \left| \sum_f N_f^c Q_f^2 y_f F_{1/2}(\tau_f) + y_W F_1(\tau_W) + Q_{H^\pm}^2 \frac{v\mu_{hH^+H^-}}{2M_{H^\pm}^2} F_0(\tau_{H^\pm}) \right|^2, \quad (3.6)$$

where  $\tau_i = M_h^2/4M_i^2$ .  $Q_f$ ,  $Q_{H^\pm}$  denote electric charges of corresponding particles.  $N_f^c$  is the color factor.  $y_f$  and  $y_W$  denote Higgs couplings to  $f\bar{f}$  and  $W^+W^-$ .  $\mu_{hH^+H^-} = \{2\lambda_4 \sin \beta \cos \beta \cos \gamma + \cos \beta^2 (\lambda_3 v_1 \cos \gamma + 4\lambda_2 v_2 \sin \gamma) + \sin \beta^2 (\lambda_4 \sin \gamma + \lambda_1 v_1 \cos \gamma + \lambda_3 v_2 \sin \gamma)\} \approx \lambda_3 v_{SM}$  stands for the coupling constant of  $hH^+H^-$  vertex. The loop functions  $F_{(0,1/2,1)}$  can be found in Ref [32].

Recently the ATLAS [33] and CMS [34] collaborations have measured the ratio of the diphoton rate  $\mu_{\gamma\gamma}$  of the observed Higgs to the SM prediction. The measured values are  $1.17 \pm 0.27$  and  $1.14_{-0.23}^{+0.26}$  in the respective experiments.

In  $\Gamma(h \rightarrow \gamma\gamma)_{\text{HTM}}$  (see eqn. 3.6), HT contributes destructively with the SM contributions for positive  $\lambda_3$  and *vice versa*. One can see from the eqn. 3.6, the contribution to the Higgs diphoton channel is proportional to  $\frac{\lambda_3}{M_{H^\pm}^2}$ . If the charged scalar mass is greater than 300 GeV then the contributions of  $H^\pm$  to the diphoton signal is negligible.

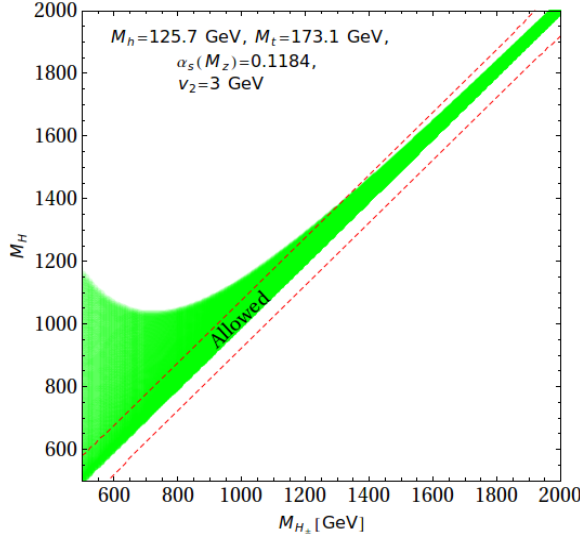


FIG. 1. The allowed mass region (green) from unitarity, perturbativity, absolute stability and experimental data of the LHC, valid upto the  $M_{\text{Pl}}$  scale. The region between the red-dashed line allowed from the EWPT data at  $2\sigma$ .

We consider that except scalar triplet  $T$ , there is no new physics between the EW scale and the Planck scale  $M_{\text{Pl}}$ . Using the renormalization group equations (RGEs), we evolve all the coupling constants of HTM ( $Y = 0$ ) from EW to Planck scale. In this work, we use the SM RGEs up to three-loop, given in Refs. [35–38] and the triplet contributions to the RGEs up to two-loop, presented in Appendix A. We show parameter spaces (green region) in Fig. 1, allowed from unitarity, perturbativity, absolute stability (see eqn. 3.1) and experimental data of the LHC, valid up to  $M_{\text{Pl}}$ . The EWPT data puts further constraints on the parameter spaces. In Fig. 1, the region between the red-dashed line is allowed from EWPT data at  $2\sigma$  C.L.

#### IV. DARK MATTER IN HTM ( $Y = 0$ )

We impose a  $\mathbb{Z}_2$ -Symmetry on the triplet scalar such that the scalar triplet is *odd* under this symmetry, i.e.,  $T \rightarrow -T$ . Whereas SM fields are even under this transformation. In the literature, the HTM with this  $\mathbb{Z}_2$ -symmetry known as inert triplet model (ITM). In this model, the term  $\lambda_4 H^\dagger \sigma^a \Phi T_a$  is absent in the scalar potential in eqn. 2.6, which implies  $\lambda_4 = 0$ . The  $\mathbb{Z}_2$ -symmetry prevents the triplet scalar to acquire VEV, i.e.,  $v_2 = 0$ . The potential can have minimum only along the Higgs field direction, i.e., the EWSB driven only by the SM Higgs doublet. The scalar fields of the triplet do not mix with the scalar fields of SM doublet. After the EWSB, the scalar

potential in eqn. 2.6 is then given by,

$$V(h, H, H^\pm) = \frac{1}{4} [2\mu_1^2(h+v)^2 + \lambda_1(h+v)^4 + 2\mu_2^2(H^2 + 2H^+H^-) + \lambda_2(H^2 + 2H^+H^-)^2 + \lambda_3(h+v)^2(H^2 + 2H^+H^-)]$$

Here,  $v \equiv v_{SM}$  and the mass (see eqn. 2.7) of these scalar fields<sup>1</sup>  $h$ ,  $H$  and  $H^\pm$  are given by,

$$\begin{aligned} M_h^2 &= \mu_1^2 + 3\lambda_1 v^2, \\ M_H^2 &= \mu_2^2 + \frac{\lambda_3}{2} v^2, \\ M_{H^\pm}^2 &= \mu_2^2 + \frac{\lambda_3}{2} v^2. \end{aligned} \tag{4.1}$$

At the tree-level mass of the neutral scalar  $H$  is same with the mass of the charged particles  $H^\pm$ . If we include one-loop radiative correction then the charged particles become slightly heavier [39, 40] than neutral ones.

$$\Delta M = (M_{H^\pm} - M_H)_{1-loop} = \frac{\alpha M_H}{4\pi s_W^2} \left[ f\left(\frac{M_W}{M_H}\right) - c_W^2 f\left(\frac{M_Z}{M_H}\right) \right],$$

$$\text{with, } f(x) = -\frac{x}{4} \left\{ 2x^3 \log(x) + (x^2 - 4)^{\frac{3}{2}} \log\left(\frac{x^2 - 2 - x\sqrt{x^2 - 4}}{2}\right) \right\}.$$

As the  $Z_2$ -symmetry also prohibits the couplings of an *odd* number of scalar fields of the triplet with the SM particles,  $H$  can serve as a viable DM candidate which may saturate the measured DM relic density of the Universe.

In Fig. 2, we have plotted the relic density as a function of DM mass for ITM. Here in this plot, we take the Higgs portal coupling  $\lambda_3(M_Z) = 0.10$ . The light red band is excluded from the Higgs invisible decay width data [41] from the LHC. The mass difference between the neutral and charged particles is  $\sim 150$  MeV for  $0.1 - 5$  TeV [39, 40]. The co-annihilation [42] cross-section of the DM  $H$  with charged scalars ( $H^\pm$ ) are very large. We see that for 500 GeV, the total cross-section is  $\langle \sigma v \rangle \sim 10^{-25} \text{ cm}^3 \text{s}^{-1}$  and so the relic density becomes  $\sim 0.01$  which corresponds to under-abundance. For DM mass greater than 1.8 TeV, we get relic density of the DM in the right ballpark. We use the software package **FeynRules** [43] along with **micrOMEGAs** [44, 45] to calculate the relic density of the DM.

Non-observation of DM signals at direct detection experiments at XENON100 [47, 48] and LUX [49] put severe restrictions [23] on the Higgs portal coupling  $\lambda_3$  for a given DM mass.

---

<sup>1</sup> The notation in eqn. 2.1 for  $v_2 = 0$ ,  $H \equiv \eta^0$  and  $H^\pm \equiv \eta^\pm$  are the physical scalar particles.

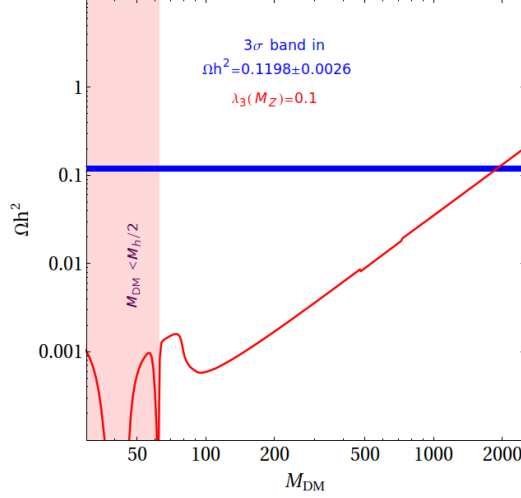


FIG. 2. Dark matter relic density  $\Omega h^2$  as a function of the DM mass  $M_{DM}(\equiv M_H)$  for the portal coupling:  $\lambda_3(M_Z) = 0.10$  (red). The thin blue band corresponds the relic density,  $\Omega h^2 = 0.1198 \pm 0.0026$  ( $3\sigma$ ) from the combined data of WMAP and Planck [46].

### A. Metastability in ITM ( $Y = 0$ )

As in the SM, the EW vacuum is metastable, it is important to explore if ITM has an answer in its reserve. As the scalar WIMP  $H$  protected by  $Z_2$ -symmetry can serve as viable DM candidate, it is interesting to explore if they help prolong the lifetime of the Universe. The effective Higgs potential gets modified in the presence of these new extra scalars.

One-loop effective Higgs potential in  $\overline{\text{MS}}$  scheme and the Landau gauge is given by

$$V_1^{\text{SM+IT}}(h) = V_1^{\text{SM}}(h) + V_1^{\text{IT}}(h)$$

where [50–54],

$$V_1^{\text{SM}}(h) = \sum_{i=1}^5 \frac{n_i}{64\pi^2} M_i^4(h) \left[ \ln \frac{M_i^2(h)}{\mu^2(t)} - c_i \right].$$

$n_i$  is the number of degrees of freedom and  $M_i^2(h) = \kappa_i(t) h^2(t) - \kappa'_i(t)$ .  $n_i$ ,  $c_i$ ,  $\kappa_i$  and  $\kappa'_i$  can be found in Eqn. (4) in Ref. [50].

The contributions to the effective Higgs potential from the new scalars ( $H, H^\pm$ ) of the inert scalar triplet is given by [13],

$$V_1^{\text{IT}}(h) = \sum_{j=H, H^+, H^-} \frac{1}{64\pi^2} M_j^4(h) \left[ \ln \left( \frac{M_j^2(h)}{\mu^2(t)} \right) - \frac{3}{2} \right], \quad (4.2)$$

where,  $M_j^2(h) = \frac{1}{2} \lambda_j(t) h^2(t) + \mu_2^2(t)$ , with  $\lambda_{H,H^\pm}(t) = \lambda_3(t)$ . In the present work, in the Higgs effective potential, SM contributions are taken at two-loop level [7, 8, 55, 56] and the IT scalar contributions are considered at one-loop only [13].

For  $h \gg v$ , the quantum corrections to the Higgs potential, are reabsorbed in the effective running coupling  $\lambda_{1,\text{eff}}$  such that the effective potential becomes,

$$V_{\text{eff}}^{\text{SM+IT}}(h) \simeq \lambda_{1,\text{eff}}(h) \frac{h^4}{4},$$

with

$$\lambda_{1,\text{eff}}(h) = \lambda_{1,\text{eff}}^{\text{SM}}(h) + \lambda_{1,\text{eff}}^{\text{IT}}(h), \quad (4.3)$$

where, the expression of  $\lambda_{1,\text{eff}}^{\text{SM}}(h)$  up to two-loop quantum corrections can be found in Ref. [7] and  $\lambda_{1,\text{eff}}^{\text{IT}}(h) = e^{4\Gamma(h)} \left[ \frac{3\lambda_3^2}{256\pi^2} \left( \ln \left( \frac{\lambda_3}{2} \right) - \frac{3}{2} \right) \right]$ , with  $\Gamma(h) = \int_{M_t}^h \gamma(\mu) d \ln \mu$ . The wave function renormalization of the Higgs field is taken care by the anomalous dimension  $\gamma(\mu)$ . Here, all running coupling constants are evaluated at  $\mu = h$ , ensuring the potential remain within the perturbative domain.

We first calculate all couplings with the threshold corrections [5–8, 57, 58] at  $M_t$ . Then we compute the RG evolution of all the couplings up to  $M_{\text{Pl}}$  using RGEs. Here, the SM effects in the RGEs are taken up to three-loop [35–38] and IT contributions are consider up to two-loop order (see appendix A).

	$\lambda_1$	$\lambda_2$	$\lambda_3$
$M_t$	0.127054	0.10	0.10
$M_{\text{Pl}}$	−0.00339962	0.267706	0.206306

TABLE I. A set of values of all quartic coupling constants at  $M_t$  and  $M_{\text{Pl}}$  for  $M_{DM} = 1897$  GeV.

We chose a specific benchmark point with  $M_{DM}(\equiv M_H) = 1897$  GeV,  $M_h = 125.7$  GeV and  $\alpha_s(M_Z) = 0.1184$  such that it reproduces the DM relic density of the Universe in the right ballpark. The corresponding values of all quartic coupling  $\lambda_{1,2,3}$  at  $M_t = 173.1$  GeV and  $M_{\text{Pl}} = 1.2 \times 10^{19}$  GeV are presented in Table I. For this benchmark point, we have shown the evolution of the running of the quartic couplings ( $\lambda_{1,2,3}$ ) in Fig. 3. We found that for this specific choice of benchmark point with the top mass<sup>2</sup>  $M_t = 173.1$  GeV and the central values of other SM parameters, the beta-function of Higgs quartic coupling  $\lambda_1$  becomes zero and  $\lambda_1$  becomes negative around the Planck scale, leading to a metastable EW vacuum. In the following subsections, we will discuss the metastability of the EW vacuum of the scalar potential.

---

<sup>2</sup> As the beta-function of Higgs quartic coupling,  $\lambda_1$  contains  $-\frac{6y_t^4}{16\pi^2}$  (see eqn. A1), the values of the Higgs quartic couplings ( $\lambda_1$ ) at very high energies are extremely sensitive to  $M_t$ .

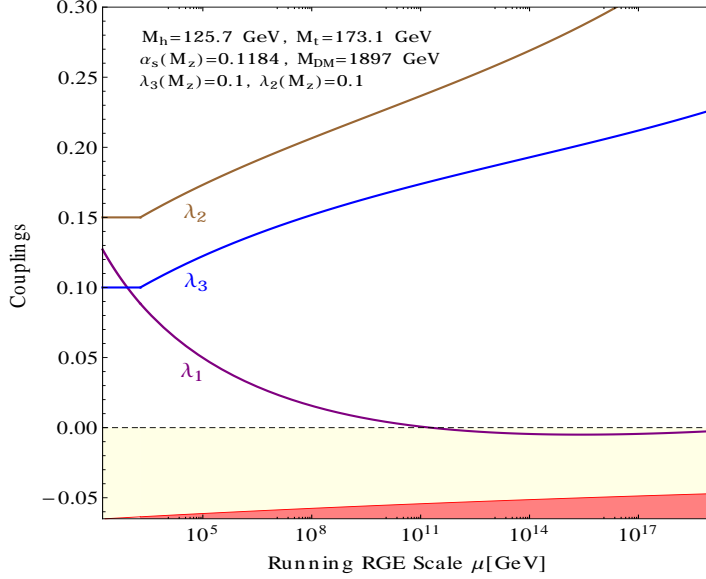


FIG. 3. *RG evolution of the couplings  $\lambda_{1,2,3}$  for the set of parameters in Table I with DM mass  $M_{DM} = 1897$  GeV.*

## B. Tunneling Probability

Using the experimentally measured values of the SM parameters at the EW scale, when analyzing the SM scalar potential at higher energy scales, one encounters with the so-called metastability of the EW vacuum [5–9]. Due to the presence of a second (true) minimum located near the Planck scale, which is much deeper than the electroweak (false) minimum, there exists a non-zero probability that the EW minimum will tunnel into the new minimum.

The tunneling probability of the EW vacuum to the true vacuum at the present epoch can be expressed as [7, 59, 60],

$$\mathcal{P}_0 = 0.15 \frac{\Lambda_B^4}{H^4} e^{-S(\Lambda_B)}, \quad (4.4)$$

where,  $S(\Lambda_B)$  is the minimum action of the Higgs potential of bounce of size  $R = \Lambda_B^{-1}$  and is given by

$$S(\Lambda_B) = \frac{8\pi^2}{3|\lambda_1(\Lambda_B)|}. \quad (4.5)$$

It becomes minimum when  $\lambda_1(\Lambda_B)$  is minimum, *i.e.*,  $\beta_{\lambda_1}(\Lambda_B) = 0$ . In this work, we neglect loop [59] and gravitational corrections [61, 62] to the action as in Ref. [5, 6]. Finite temperature also affects to EW vacuum stability [59, 63, 64]. In this work, we consider field theory at the zero-temperature limit.

In the ITM, the additional scalar fields give a positive contribution to  $\beta_{\lambda_1}$  (see Eqns. A1, A2). Due to the presence of these extra scalars, a metastable EW vacuum goes towards the stability, i.e., the tunneling probability  $\mathcal{P}_0$  become lower. We have first calculated the minimum value of  $\lambda_{1,\text{eff}}$  of eqn. 4.3. Putting this minimum value in eqn. 4.5, we calculate the tunneling probability  $\mathcal{P}_0$  (see eqn. 4.4). As the stability of the EW vacuum is very sensitive to the top mass  $M_t$ , we have shown the variation of tunneling probability  $\mathcal{P}_0$  as a function of  $M_t$  in Fig. 4(a). The right band in Fig. 4(a) corresponds to the tunneling probability for our benchmark point. We have also presented  $\mathcal{P}_0$  for SM as the left band to see the effect of IT scalar for our bench mark point.  $1\sigma$  error bands in  $\alpha_s$  (light-grey) and  $M_h$  (light-red) are also displayed. One can see from this figure that the effect of  $\alpha_s$  on the tunneling probability is significant than the effect of  $M_h$ . To see the effect of ITM parameter spaces, we plot  $\mathcal{P}_0$  as a function of Higgs portal coupling  $\lambda_3(M_Z)$  in Fig. 4(b) for different choices of  $\lambda_2(M_Z)$ , assuming central values for the SM-parameters. Here, DM mass  $M_{DM}$  is also varied with  $\lambda_3$  to get DM relic density  $\Omega h^2 = 0.1198$ .

In the addition of extra scalar fields of  $SU(2)$  triplet with the SM improves the stability conditions of the EW vacuum as,

- If  $0 > \lambda_1(\Lambda_B) > \lambda_{1,\text{min}}(\Lambda_B)$ , then the vacuum is metastable.
- If  $\lambda_1(\Lambda_B) < \lambda_{1,\text{min}}(\Lambda_B)$ , then the vacuum is unstable.
- If  $\lambda_2 < 0$ , the potential is unbounded from below along the  $H$  and  $H^\pm$ -direction.
- If  $\lambda_3(\Lambda_I) < 0$ , the potential is unbounded from below along a direction in between  $H$  and  $h$  also  $H^\pm$  and  $h$ .

In the above  $\lambda_{1,\text{min}}(\Lambda_B) = \frac{-0.06488}{1-0.00986 \ln(v/\Lambda_B)}$  and  $\Lambda_I$  represents any energy scale for which  $\lambda_1$  is negative [5, 6].

### C. Phase diagrams

In order to show the explicit dependence of the electroweak stability on different parameters of ITM, we present various kinds of phase diagrams. Graphical demonstrations have been provided to illustrate how the confidence level, at which stability of EW vacuum is excluded, depends on such new physics parameters. In Fig. 5 phase diagram in  $M_t - M_h$  and  $\alpha_s(M_Z) - M_t$  plane has been presented for the benchmark points  $M_{DM} = 1897$  GeV,  $\lambda_2(M_Z) = 0.10$  and  $\lambda_3(M_Z) = 0.10$ . For this points one can see from the phase diagram in Fig. 5 that the stability EW vacuum is excluded at  $1.2\sigma$  (one-sided).

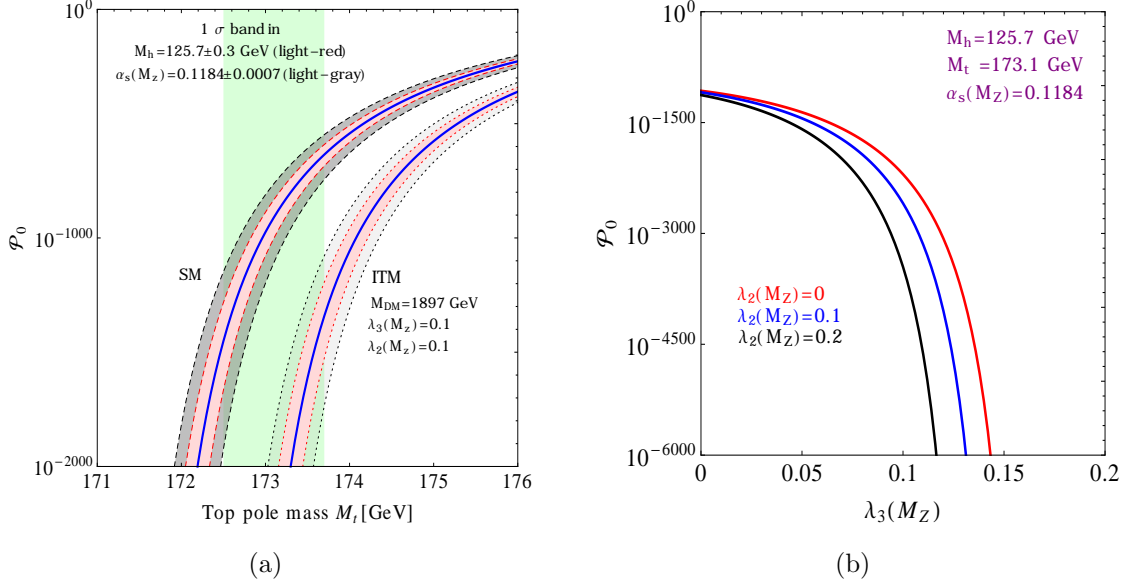


FIG. 4. (a) Tunneling probability  $\mathcal{P}_0$  dependence on  $M_t$ . The left band (between dashed lines) corresponds to SM. The right one (between dotted lines) is for IT model for DM mass  $M_H = 1897$  GeV. Dark matter constraints are respected for these specific choice of parameters. Light-green band stands for  $M_t$  at  $\pm 1\sigma$ . (b)  $\mathcal{P}_0$  is plotted against Higgs DM coupling  $\lambda_S(M_Z)$  for different values of  $\lambda_2(M_Z)$ .

If the ITM is valid up to the Planck scale, which saturates the relic abundance of the DM of the Universe then the confidence level vs  $\lambda_3(M_Z)$  phase diagram becomes important to realize where the present EW vacuum is residing. Along the line (black, blue and red) in the Fig. 6 the DM mass change in such a way that the relic density  $\Omega h^2 = 0.1198$  remains same. One can see that with the increase of  $\lambda_{2,3}(M_Z)$ , the EW vacuum approaches the stability. The EW vacuum becomes absolutely stable after  $\lambda_3(M_Z) = 0.154$  for  $\lambda_2(M_Z) \approx 0.10$  (see blue line if the Fig. 6). This phase diagram has been presented for central values of  $M_h$ ,  $M_t$  and  $\alpha_s(M_Z)$ . However, if we increase the top mass or decrease the Higgs mass or decrease  $\alpha_s(M_Z)$  within experimental uncertainties then the size of the region corresponding to the metastability of the EW vacuum increases. With a maximum top mass  $M_t = 174.9$  GeV and a minimum  $M_h = 124.8$  GeV and a minimum  $\alpha_s(M_Z) = 0.1163$ , allowed at  $3\sigma$ , the EW vacuum the Higgs potential becomes absolutely stable for the DM mass more than 1912 GeV with  $\lambda_3(M_Z)$  greater than 0.31 for fixed  $\lambda_2(M_Z) = 0.1$ .

In Fig. 7, we have shown the valid parameter spaces in  $\lambda_3(M_Z) - M_{H^\pm}$  plane for central value of  $M_t$ ,  $M_h$  and  $\alpha(M_Z)$  with  $\lambda_2(M_Z) = 0.1$ . Here the lower (red) region are excluded, as the scalar potential becomes unbounded from below along the direction in between  $H^\pm$  and  $h$ . In this region, the effective Higgs quartic coupling is negative and form a local minimum along the Higgs  $h$  direction near the Planck scale and at the same time  $\lambda_3$  are remains negative up to the Planck



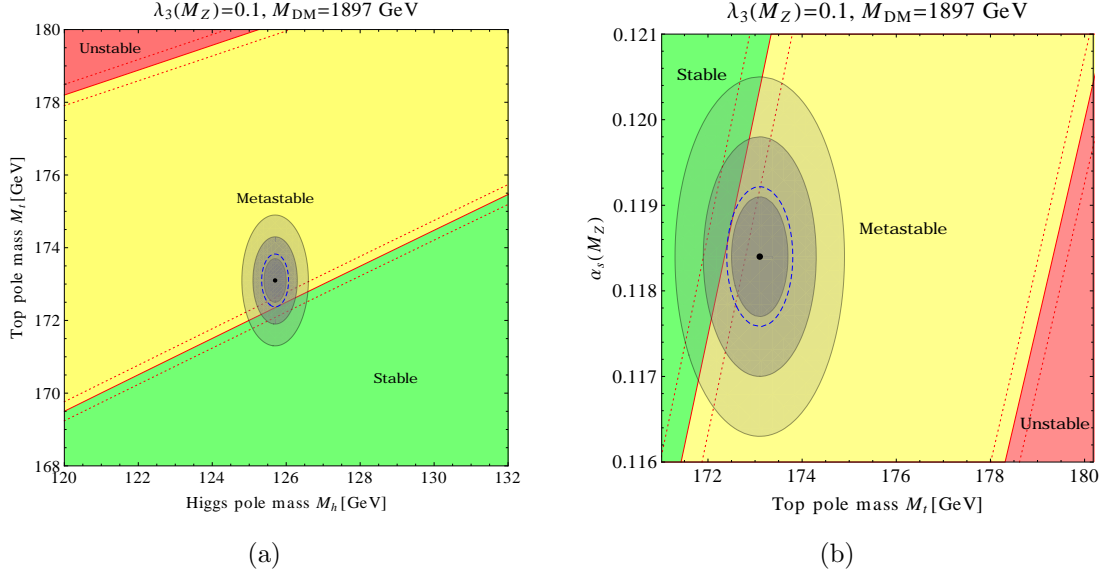


FIG. 5. Phase diagrams in (a)  $M_h - M_t$  plane and (b)  $M_t - \alpha_s(M_Z)$  plane ITM. Regions of absolute stability (green), metastability (yellow), instability (red) of the EW vacuum are also marked. The gray zones represent error ellipses at 1, 2 and  $3\sigma$ . The three boundary lines (dotted, solid and dotted red) correspond to  $\alpha_s(M_Z) = 0.1184 \pm 0.0007$ .

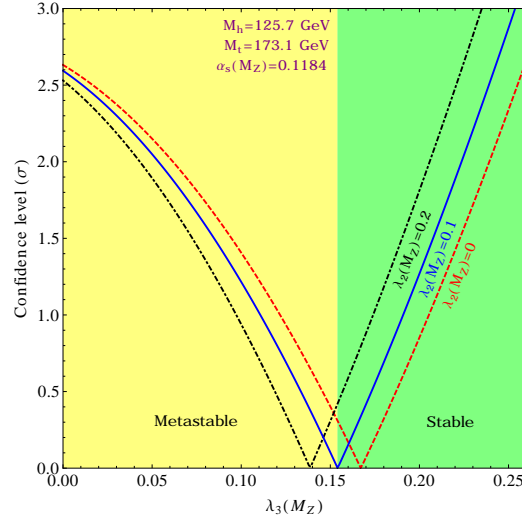


FIG. 6. Dependence of confidence level at which EW vacuum stability is excluded (one-sided) or allowed on  $\lambda_3(M_Z)$  and  $\lambda_2(M_Z)$  in ITM. Regions of absolute stability (green) and metastability (yellow) of EW vacuum are shown for  $\lambda_2(M_Z) = 0.1$ .

scale. It has been found that the parameter spaces with negative  $\lambda_3(M_Z)$  are also allowed from the metastability. In this case,  $\lambda_3$  becomes positive at the scale  $\Lambda_B$  of global minimum and remains positive up to the Planck scale. The green region implies that the EW vacuum is absolutely stable. In the upper red region the unitary bounds are violated. In this plot, the right-side of the black dotted line are viable from  $\mu_{\gamma\gamma}$  at  $1\sigma$ .

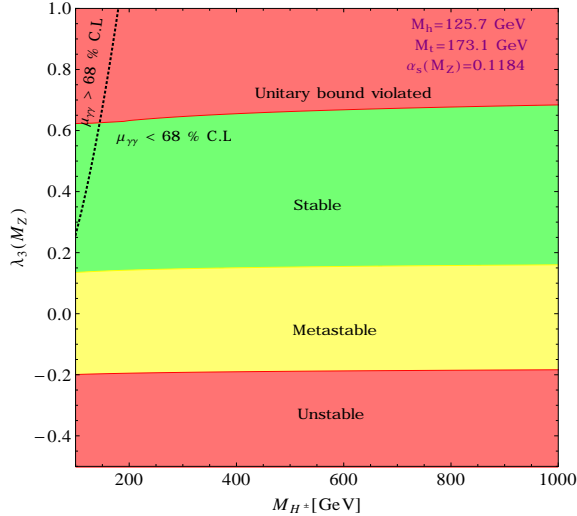


FIG. 7. Phase diagram in  $\lambda_3(M_Z) - M_{H^\pm}$  plane in ITM. Right side of the black-dotted line is allowed from the signal strength ratio of  $\mu_{\gamma\gamma}$  within 68% confidence level and the left side is excluded at  $1\sigma$ . In the metastable region, the Higgs portal coupling  $\lambda_3(M_Z)$  is negative, however, beyond the scale  $\Lambda_B$  it is greater than zero.

## V. DISCUSSION AND CONCLUSIONS

The measurements of the properties of the Higgs-like scalar boson detected at the Large Hadron Collider on 4th July 2012, are consistent with the minimal choice of the scalar sector. But the experimental data of the Higgs signal strengths and the uncertainties in the measurement of other standard model parameters still allow an extended scalar sector. We have considered an extra hyperchargeless scalar triplet as a new physics with the SM. First, we consider the extra neutral  $CP$ -even component of the scalar triplet also participated in the EWSB. We have shown the detailed structure of the tree-level scalar potential and mixing of the scalar fields. We have also discussed the bounds on the VEV ( $v_2$ ) of the neutral  $CP$ -even component of the scalar triplet from the  $\rho$ -parameter. To the best of our knowledge, the full expressions of unitarity bounds on the quartic couplings of the scalar potential in this model have not yet been presented in the

literature. We have shown for the first time the unitarity bounds in this model. As the SM gauge symmetry  $SU(2)_L$  prohibits the coupling of SM neutrinos with the neutral  $CP$ -even component ( $\eta^0$ ) of the scalar triplet, the model does not give neutrino masses. But the model still interesting as it can play the role in improving the stability of the Higgs potential. Using the SM RGEs up to three-loop and the triplet contributions to the RGEs up to two-loop, first time we have shown the parameter spaces in the  $M_{H^\pm} - M_H$  plane which is allowed from unitarity, perturbativity, absolute stability and from the LHC and the EWPT data, valid up to the Planck scale  $M_{\text{Pl}}$ .

Various kinds of astrophysical observations, e.g., anomalies in the galactic rotation curves, gravitational lensing effects in Bullet cluster etc., have indicated the existence of DM in the Universe. In the ITM, the extra scalar fields are protected by a discrete  $Z_2$ -symmetry that ensures the stability of the lightest neutral particle. We have verified that the mass of the neutral scalar particle ( $H$ ) are slightly lighter than the mass of the charged particle ( $H^\pm$ ) then the contributions coming from co-annihilation between  $H$  and  $H^\pm$  play a significant role in relic density calculation. Due to large co-annihilation rate, the relic density of the dark matter found is in under-abundance for the low DM mass. We get the relic density in the right ballpark for DM mass greater than 1.8 TeV. In this context, we have shown how the presence of an additional hyperchargeless scalar triplet improves the stability of the Higgs potential. In this study, we have used state of the art next-to-next-to leading order (NNLO) for the SM calculations, i.e., the Higgs scalar potential up to two-loop quantum corrections is used and it is improved by three-loop renormalization group running of the coupling parameters. Whereas the contributions to the effective Higgs potential from these new scalars has been taken at one-loop level only. These contributions are improved by two-loop renormalization group running of the new parameters. In this paper, we explored the stability of the EW minimum of the new effective Higgs potential in the ITM up to the Planck scale. We have shown the new modified stability conditions in this model when EW vacuum still remains metastable. To see the explicit dependence of various parameters on EW stability, we have presented various phase diagrams in various parameter spaces. We have identified for the first time new parameter spaces in ITM that correspond to the stable and metastable EW vacuum, which also saturates the relic density of the DM of the Universe as measured by the WMAP and Planck experiments.

### Acknowledgements:

The work of N.K. is supported by a fellowship from University Grants Commission. This work is partially supported by a grant from the Department of Science and Technology, India via Grant No. EMR/2014/001177. I would like to thank Subhendu Rakshit, Amitava Raychaudhuri and Amitava Datta for useful discussions.

## Appendix A: Two-loop beta functions for IT Model

The beta functions of the coupling ( $\chi_i = \lambda_{1,2,3,4}$ ) parameters for the HTM ( $Y = 0$ ) model are defined as

$$\beta_{\chi_i} = \frac{\partial \chi_i}{\partial \ln \mu} = \frac{1}{16\pi^2} \beta_{\chi_i}^{(1)} + \frac{1}{(16\pi^2)^2} \beta_{\chi_i}^{(2)}.$$

For  $\mu < M_H$ ,

$$\beta_{\lambda_1} = \beta_{\lambda}^{SM} \quad \text{and} \quad \beta_{\lambda_{2,3}} = 0,$$

and for  $\mu > M_H$ ,

$$\begin{aligned} \beta_{\lambda_1}^{(1)} = & +\frac{27}{200}g_1^4 + \frac{9}{20}g_1^2g_2^2 + \frac{9}{8}g_2^4 - \frac{9}{5}g_1^2\lambda_1 - 9g_2^2\lambda_1 + 24\lambda_1^2 + \frac{3}{2}\lambda_3^2 + 12\lambda_1\text{Tr}(Y_dY_d^\dagger) + 4\lambda_1\text{Tr}(Y_eY_e^\dagger) \\ & + 12\lambda_1\text{Tr}(Y_uY_u^\dagger) - 6\text{Tr}(Y_dY_d^\dagger Y_dY_d^\dagger) - 2\text{Tr}(Y_eY_e^\dagger Y_eY_e^\dagger) - 6\text{Tr}(Y_uY_u^\dagger Y_uY_u^\dagger) \end{aligned} \quad (\text{A1})$$

$$\begin{aligned} \beta_{\lambda_1}^{(2)} = & -\frac{3411}{2000}g_1^6 - \frac{1677}{400}g_1^4g_2^2 - \frac{317}{80}g_1^2g_2^4 + \frac{277}{16}g_2^6 + \frac{1887}{200}g_1^4\lambda_1 + \frac{117}{20}g_1^2g_2^2\lambda_1 - \frac{29}{8}g_2^4\lambda_1 + \frac{108}{5}g_1^2\lambda_1^2 \\ & + 108g_2^2\lambda_1^2 - 312\lambda_1^3 + 5g_2^4\lambda_3 + 12g_2^2\lambda_3^2 - 15\lambda_1\lambda_3^2 - 2\lambda_3^3 \\ & + \frac{1}{20}\left(-5\left(64\lambda_1\left(-5g_2^2 + 9\lambda_1\right) - 90g_2^2\lambda_1 + 9g_2^4\right) + 9g_1^4 + g_1^2\left(50\lambda_1 + 54g_2^2\right)\right)\text{Tr}(Y_dY_d^\dagger) \\ & - \frac{3}{20}\left(15g_1^4 - 2g_1^2\left(11g_2^2 + 25\lambda_1\right) + 5\left(-10g_2^2\lambda_1 + 64\lambda_1^2 + g_2^4\right)\right)\text{Tr}(Y_eY_e^\dagger) - \frac{171}{100}g_1^4\text{Tr}(Y_uY_u^\dagger) \\ & + \frac{63}{10}g_1^2g_2^2\text{Tr}(Y_uY_u^\dagger) - \frac{9}{4}g_2^4\text{Tr}(Y_uY_u^\dagger) + \frac{17}{2}g_1^2\lambda_1\text{Tr}(Y_uY_u^\dagger) + \frac{45}{2}g_2^2\lambda_1\text{Tr}(Y_uY_u^\dagger) \\ & + 80g_3^2\lambda_1\text{Tr}(Y_uY_u^\dagger) - 144\lambda_1^2\text{Tr}(Y_uY_u^\dagger) + \frac{4}{5}g_1^2\text{Tr}(Y_dY_d^\dagger Y_dY_d^\dagger) - 32g_3^2\text{Tr}(Y_dY_d^\dagger Y_dY_d^\dagger) \\ & - 3\lambda_1\text{Tr}(Y_dY_d^\dagger Y_dY_d^\dagger) - 42\lambda_1\text{Tr}(Y_dY_u^\dagger Y_uY_d^\dagger) - \frac{12}{5}g_1^2\text{Tr}(Y_eY_e^\dagger Y_eY_e^\dagger) - \lambda_1\text{Tr}(Y_eY_e^\dagger Y_eY_e^\dagger) \\ & - \frac{8}{5}g_1^2\text{Tr}(Y_uY_u^\dagger Y_uY_u^\dagger) - 32g_3^2\text{Tr}(Y_uY_u^\dagger Y_uY_u^\dagger) - 3\lambda_1\text{Tr}(Y_uY_u^\dagger Y_uY_u^\dagger) + 30\text{Tr}(Y_dY_d^\dagger Y_dY_d^\dagger Y_dY_d^\dagger) \\ & + 6\text{Tr}(Y_dY_d^\dagger Y_dY_u^\dagger Y_uY_d^\dagger) - 12\text{Tr}(Y_dY_u^\dagger Y_uY_d^\dagger Y_dY_d^\dagger) - 6\text{Tr}(Y_dY_u^\dagger Y_uY_u^\dagger Y_uY_d^\dagger) \\ & + 10\text{Tr}(Y_eY_e^\dagger Y_eY_e^\dagger Y_eY_e^\dagger) + 30\text{Tr}(Y_uY_u^\dagger Y_uY_u^\dagger Y_uY_u^\dagger) \end{aligned} \quad (\text{A2})$$

$$\beta_{\lambda_2}^{(1)} = 2\left(11\lambda_2^2 - 12g_2^2\lambda_2 + 3g_2^4 + \lambda_3^2\right) \quad (\text{A3})$$

$$\begin{aligned} \beta_{\lambda_2}^{(2)} = & -\frac{272}{3}g_2^6 + \frac{94}{3}g_2^4\lambda_2 + 160g_2^2\lambda_2^2 - 244\lambda_2^3 + 10g_2^4\lambda_3 + \frac{12}{5}g_1^2\lambda_3^2 + 12g_2^2\lambda_3^2 - 20\lambda_2\lambda_3^2 - 8\lambda_3^3 \\ & - 12\lambda_3^2\text{Tr}(Y_dY_d^\dagger) - 4\lambda_3^2\text{Tr}(Y_eY_e^\dagger) - 12\lambda_3^2\text{Tr}(Y_uY_u^\dagger) \end{aligned} \quad (\text{A4})$$

$$\beta_{\lambda_3}^{(1)} = +3g_2^4 - \frac{9}{10}g_1^2\lambda_3 - \frac{33}{2}g_2^2\lambda_3 + 12\lambda_1\lambda_3 + 10\lambda_2\lambda_3 + 4\lambda_3^2 + 6\lambda_3\text{Tr}(Y_dY_d^\dagger) + 2\lambda_3\text{Tr}(Y_eY_e^\dagger)$$

$$+ 6\lambda_3 \text{Tr}(Y_u Y_u^\dagger) \quad (\text{A5})$$

$$\begin{aligned} \beta_{\lambda_3}^{(2)} = & -\frac{9}{4}g_1^2g_2^4 + \frac{329}{12}g_2^6 + 30g_2^4\lambda_1 + 20g_2^4\lambda_2 + \frac{1671}{400}g_1^4\lambda_3 + \frac{9}{8}g_1^2g_2^2\lambda_3 - \frac{607}{48}g_2^4\lambda_3 + \frac{72}{5}g_1^2\lambda_1\lambda_3 \\ & + 72g_2^2\lambda_1\lambda_3 - 60\lambda_1^2\lambda_3 + 88g_2^2\lambda_2\lambda_3 - 34\lambda_2^2\lambda_3 + \frac{3}{5}g_1^2\lambda_3^2 + 11g_2^2\lambda_3^2 - 72\lambda_1\lambda_3^2 - 52\lambda_2\lambda_3^2 \\ & - \frac{23}{2}\lambda_3^3 + \left(-12\lambda_3^2 - 3g_2^4 + 40g_3^2\lambda_3 - 72\lambda_1\lambda_3 + \frac{45}{4}g_2^2\lambda_3 + \frac{5}{4}g_1^2\lambda_3\right)\text{Tr}(Y_d Y_d^\dagger) \\ & - \frac{1}{4}\left(4g_2^4 + \lambda_3(16\lambda_3 + 96\lambda_1 - 15g_2^2 - 15g_1^2)\right)\text{Tr}(Y_e Y_e^\dagger) - 3g_2^4\text{Tr}(Y_u Y_u^\dagger) + \frac{17}{4}g_1^2\lambda_3\text{Tr}(Y_u Y_u^\dagger) \\ & + \frac{45}{4}g_2^2\lambda_3\text{Tr}(Y_u Y_u^\dagger) + 40g_3^2\lambda_3\text{Tr}(Y_u Y_u^\dagger) - 72\lambda_1\lambda_3\text{Tr}(Y_u Y_u^\dagger) - 12\lambda_3^2\text{Tr}(Y_u Y_u^\dagger) \\ & - \frac{27}{2}\lambda_3\text{Tr}(Y_d Y_d^\dagger Y_d Y_d^\dagger) - 21\lambda_3\text{Tr}(Y_d Y_u^\dagger Y_u Y_d^\dagger) - \frac{9}{2}\lambda_3\text{Tr}(Y_e Y_e^\dagger Y_e Y_e^\dagger) - \frac{27}{2}\lambda_3\text{Tr}(Y_u Y_u^\dagger Y_u Y_u^\dagger) \end{aligned} \quad (\text{A6})$$

$$\beta_{\lambda_4}^{(1)} = 2\lambda_4\text{Tr}(Y_e Y_e^\dagger) + 4\lambda_1\lambda_4 + 4\lambda_3\lambda_4 + 6\lambda_4\text{Tr}(Y_d Y_d^\dagger) + 6\lambda_4\text{Tr}(Y_u Y_u^\dagger) - \frac{21}{2}g_2^2\lambda_4 - \frac{9}{10}g_1^2\lambda_4 \quad (\text{A7})$$

$$\begin{aligned} \beta_{\lambda_4}^{(2)} = & +\frac{1311}{400}g_1^4\lambda_4 + \frac{141}{40}g_1^2g_2^2\lambda_4 - \frac{1343}{48}g_2^4\lambda_4 + \frac{24}{5}g_1^2\lambda_1\lambda_4 - 28\lambda_1^2\lambda_4 + 5\lambda_2^2\lambda_4 + \frac{3}{5}g_1^2\lambda_3\lambda_4 \\ & + 23g_2^2\lambda_3\lambda_4 - 40\lambda_1\lambda_3\lambda_4 - 20\lambda_2\lambda_3\lambda_4 - \frac{17}{2}\lambda_3^2\lambda_4 + \frac{\lambda_4}{4}\left(160g_3^2 + 45g_2^2 - 48\lambda_3 + 5g_1^2\right. \\ & \left.- 96\lambda_1\right)\text{Tr}(Y_d Y_d^\dagger) + \frac{1}{4}\left(15g_1^2 + 15g_2^2 - 16(2\lambda_1 + \lambda_3)\right)\lambda_4\text{Tr}(Y_e Y_e^\dagger) \\ & + \frac{17}{4}g_1^2\lambda_4\text{Tr}(Y_u Y_u^\dagger) + \frac{45}{4}g_2^2\lambda_4\text{Tr}(Y_u Y_u^\dagger) + 40g_3^2\lambda_4\text{Tr}(Y_u Y_u^\dagger) - 24\lambda_1\lambda_4\text{Tr}(Y_u Y_u^\dagger) \\ & - 12\lambda_3\lambda_4\text{Tr}(Y_u Y_u^\dagger) - \frac{27}{2}\lambda_4\text{Tr}(Y_d Y_d^\dagger Y_d Y_d^\dagger) + 27\lambda_4\text{Tr}(Y_d Y_u^\dagger Y_u Y_d^\dagger) - \frac{9}{2}\lambda_4\text{Tr}(Y_e Y_e^\dagger Y_e Y_e^\dagger) \\ & - \frac{27}{2}\lambda_4\text{Tr}(Y_u Y_u^\dagger Y_u Y_u^\dagger) \end{aligned} \quad (\text{A8})$$

Two-loop RGEs used in this work have been generated using **SARAH** [65]. Here,  $Y_u = y_u, y_c, y_t$  are the Yukawa couplings of up-,charm- and top-quark,  $Y_d = y_d, y_s, y_b$  for down-, strange and bottom-quark.  $Y_e$  represents for charged leptons. In our work, we have taken only the top-quark contributions. The other Yukawa couplings are very small, it does not alter our result.

- 
- [1] G. Aad *et al.* [ATLAS Collaboration], Phys. Lett. B **716**, 1 (2012) [arXiv:1207.7214 [hep-ex]].
  - [2] S. Chatrchyan *et al.* [CMS Collaboration], Phys. Lett. B **716**, 30 (2012) [arXiv:1207.7235 [hep-ex]].
  - [3] P. P. Giardino, K. Kannike, I. Masina, M. Raidal and A. Strumia, JHEP **1405**, 046 (2014) [arXiv:1303.3570 [hep-ph]].
  - [4] CMS Collaboration, CMS-PAS-HIG-15-002 (2015).
  - [5] N. Khan and S. Rakshit, Phys. Rev. D **90**, 113008 (2014) [arXiv:1407.6015 [hep-ph]].
  - [6] N. Khan and S. Rakshit, Phys. Rev. D **92**, 055006 (2015) [arXiv:1503.03085 [hep-ph]].
  - [7] D. Buttazzo, G. Degrassi, P. P. Giardino, G. F. Giudice, F. Sala, A. Salvio and A. Strumia, JHEP **1312**, 089 (2013) [arXiv:1307.3536].
  - [8] G. Degrassi, S. Di Vita, J. Elias-Miro, J. R. Espinosa, G. F. Giudice, G. Isidori and A. Strumia, JHEP **1208**, 098 (2012) [arXiv:1205.6497 [hep-ph]].
  - [9] I. Masina, Phys. Rev. D **87**, 053001 (2013) [arXiv:1209.0393 [hep-ph]].
  - [10] J. Elias-Miro, J. R. Espinosa, G. F. Giudice, G. Isidori, A. Riotto and A. Strumia, Phys. Lett. B **709**, 222 (2012) [arXiv:1112.3022 [hep-ph]].
  - [11] T. Blank and W. Hollik, Nucl. Phys. B **514**, 113 (1998) [hep-ph/9703392].
  - [12] N. Khan, B. Mukhopadhyaya, S. Rakshit and A. Shaw, arXiv:1608.05673 [hep-ph].
  - [13] J. R. Forshaw, A. Sabio Vera and B. E. White, JHEP **0306**, 059 (2003) [hep-ph/0302256].
  - [14] M. C. Chen, S. Dawson and C. B. Jackson, Phys. Rev. D **78**, 093001 (2008) [arXiv:0809.4185 [hep-ph]].
  - [15] M. C. Chen, S. Dawson and T. Krupovnickas, Phys. Rev. D **74**, 035001 (2006) [hep-ph/0604102].
  - [16] M. C. Chen, S. Dawson and T. Krupovnickas, Int. J. Mod. Phys. A **21**, 4045 (2006) [hep-ph/0504286].
  - [17] P. H. Chankowski, S. Pokorski and J. Wagner, Eur. Phys. J. C **50**, 919 (2007) [hep-ph/0605302].
  - [18] J. R. Forshaw, D. A. Ross and B. E. White, JHEP **0110**, 007 (2001) [hep-ph/0107232].
  - [19] P. Fileviez Perez, H. H. Patel, M. J. Ramsey-Musolf and K. Wang, Phys. Rev. D **79**, 055024 (2009) [arXiv:0811.3957 [hep-ph]].
  - [20] L. Wang and X. F. Han, JHEP **1403**, 010 (2014) [arXiv:1303.4490 [hep-ph]].
  - [21] S. Y. Ayazi and S. M. Firouzabadi, arXiv:1501.06176 [hep-ph].
  - [22] T. Araki, C. Q. Geng and K. I. Nagao, Phys. Rev. D **83**, 075014 (2011) [arXiv:1102.4906 [hep-ph]].
  - [23] S. Y. Ayazi and S. M. Firouzabadi, JCAP **1411**, 005 (2014) [arXiv:1408.0654 [hep-ph]].
  - [24] F. X. Josse-Michaux and E. Molinaro, Phys. Rev. D **87**, 036007 (2013) [arXiv:1210.7202 [hep-ph]].
  - [25] K. A. Olive *et al.* [Particle Data Group Collaboration], Chin. Phys. C **38**, 090001 (2014).
  - [26] B. W. Lee, C. Quigg and H. B. Thacker, Phys. Rev. D **16**, 1519 (1977).
  - [27] Y. P. Yao and C. P. Yuan, Phys. Rev. D **38**, 2237 (1988); H. G. J. Veltman, Phys. Rev. D **41**, 2294 (1990).

- (1990); H. J. He *et al.*, Phys. Rev. Lett. **69**, 2619 (1992).
- [28] S. Kanemura *et al.*, Phys. Lett. B **313**, 155-160 (1993).
  - [29] A. Arhrib, hep-ph/0012353.
  - [30] M. E. Peskin and T. Takeuchi, Phys. Rev. D **46**, 381 (1992).
  - [31] M. Baak *et al.* [Gfitter Group Collaboration], Eur. Phys. J. C **74**, 3046 (2014) [arXiv:1407.3792 [hep-ph]].
  - [32] A. Djouadi, Phys. Rept. **459**, 1 (2008) [hep-ph/0503173].
  - [33] G. Aad *et al.* [ATLAS Collaboration], Phys. Rev. D **90**, 112015 (2014) [arXiv:1408.7084 [hep-ex]].
  - [34] V. Khachatryan *et al.* [CMS Collaboration], Eur. Phys. J. C **74**, 3076 (2014) [arXiv:1407.0558 [hep-ex]].
  - [35] K. G. Chetyrkin and M. F. Zoller, JHEP **1206**, 033 (2012) [arXiv:1205.2892 [hep-ph]].
  - [36] M. F. Zoller, arXiv:1209.5609 [hep-ph].
  - [37] K. G. Chetyrkin and M. F. Zoller, JHEP **1304**, 091 (2013), [Erratum-ibid. **1309**, 155 (2013)] [arXiv:1303.2890 [hep-ph]].
  - [38] M. Zoller, PoS EPS-HEP2013, 322 (2014) [arXiv:1311.5085 [hep-ph]].
  - [39] M. Cirelli, N. Fornengo and A. Strumia, Nucl. Phys. B **753**, 178 (2006) [hep-ph/0512090].
  - [40] M. Cirelli and A. Strumia, New J. Phys. **11**, 105005 (2009) [arXiv:0903.3381 [hep-ph]].
  - [41] G. Belanger, B. Dumont, U. Ellwanger, J. F. Gunion and S. Kraml, Phys. Rev. D **88**, 075008 (2013) [arXiv:1306.2941 [hep-ph]].
  - [42] K. Griest and D. Seckel, Phys. Rev. D **43**, 3191 (1991).
  - [43] A. Alloul, N. D. Christensen, C. Degrande, C. Duhr and B. Fuks, Comput. Phys. Commun. **185**, 2250 (2014) [arXiv:1310.1921 [hep-ph]].
  - [44] G. Belanger, F. Boudjema, P. Brun, A. Pukhov, S. Rosier-Lees, P. Salati and A. Semenov, Comput. Phys. Commun. **182**, 842 (2011) [arXiv:1004.1092 [hep-ph]].
  - [45] G. Belanger, F. Boudjema, A. Pukhov and A. Semenov, Comput. Phys. Commun. **185**, 960 (2014) [arXiv:1305.0237 [hep-ph]].
  - [46] P. A. R. Ade *et al.* [Planck Collaboration], arXiv:1303.5076 [astro-ph.CO].
  - [47] E. Aprile *et al.* [XENON100 Collaboration], Phys. Rev. Lett. **107**, 131302 (2011) [arXiv:1104.2549 [astro-ph.CO]].
  - [48] E. Aprile *et al.* [XENON100 Collaboration], Phys. Rev. Lett. **109**, 181301 (2012) [arXiv:1207.5988 [astro-ph.CO]].
  - [49] D. S. Akerib *et al.* [LUX Collaboration], Phys. Rev. Lett. **112**, 091303 (2014) [arXiv:1310.8214 [astro-ph.CO]].
  - [50] J. A. Casas, J. R. Espinosa and M. Quiros, Phys. Lett. B **342**, 171 (1995) [hep-ph/9409458].
  - [51] G. Altarelli and G. Isidori, Phys. Lett. B **337**, 141 (1994).
  - [52] J. A. Casas, J. R. Espinosa, M. Quiros and A. Riotto, Nucl. Phys. B **436**, 3 (1995), [Erratum-ibid.

- B **439**, 466 (1995)] [hep-ph/9407389].
- [53] J. A. Casas, J. R. Espinosa and M. Quiros, Phys. Lett. B **382**, 374 (1996) [hep-ph/9603227].
  - [54] M. Quiros, hep-ph/9703412.
  - [55] C. Ford, I. Jack and D. R. T. Jones, Nucl. Phys. B **387**, 373 (1992), [Erratum-ibid. B **504**, 551 (1997)] [hep-ph/0111190].
  - [56] S. P. Martin, Phys. Rev. D **65**, 116003 (2002) [hep-ph/0111209].
  - [57] A. Sirlin and R. Zucchini, Nucl. Phys. B **266**, 389 (1986).
  - [58] F. Bezrukov, M. Y. Kalmykov, B. A. Kniehl and M. Shaposhnikov, JHEP **1210**, 140 (2012) [arXiv:1205.2893 [hep-ph]].
  - [59] G. Isidori, G. Ridolfi and A. Strumia, Nucl. Phys. B **609**, 387 (2001) [hep-ph/0104016].
  - [60] S. R. Coleman, Phys. Rev. D **15**, 2929 (1977), [Erratum-ibid. D **16**, 1248 (1977)].
  - [61] S. R. Coleman and F. De Luccia, Phys. Rev. D **21**, 3305 (1980).
  - [62] G. Isidori, V. S. Rychkov, A. Strumia and N. Tetradis, Phys. Rev. D **77**, 025034 (2008) [arXiv:0712.0242 [hep-ph]].
  - [63] L. Delle Rose, C. Marzo and A. Urbano, JHEP **1605**, 050 (2016) [arXiv:1507.06912 [hep-ph]].
  - [64] J. R. Espinosa and M. Quiros, Phys. Lett. B **353**, 257 (1995) [hep-ph/9504241].
  - [65] F. Staub, Comput. Phys. Commun. **185**, 1773 (2014) [arXiv:1309.7223 [hep-ph]]; F. Staub, arXiv:1503.04200 [hep-ph].